Virologica Sinica 40 (2025) 275–283

Contents lists available at ScienceDirect

Virologica Sinica

journal homepage: www.keaipublishing.com/en/journals/virologica-sinica
www.virosin.org

Research Article

Development of a reporter HBoV1 strain for antiviral drug screening and life cycle studies

Jielin Tang [a,b,*,1], Sijie Chen [a,b,1], Yi Zhong [a], Yijun Deng [a,b], Dan Huang [a,c], Junjun Liu [a], Yi Zheng [c], Jiyuan Xu [a,c], Bao Xue [a,c], Fan Wang [d], Yuan Zhou [a], Hanzhong Wang [c], Qi Yang [a,b,*], Xinwen Chen [a,b]

[a] Guangzhou National Laboratory, Guangzhou 510005, China
[b] State Key Laboratory of Respiratory Disease, The First Affiliated Hospital of Guangzhou Medical University, Guangzhou 511436, China
[c] State Key Laboratory of Virology, Wuhan Institute of Virology, Center for Biosafety Mega-Science, Chinese Academy of Sciences, Wuhan 430071, China
[d] GMU-GIBH Joint School of Life Sciences, Guangzhou Medical University, Guangzhou 511436, China

ARTICLE INFO

Keywords:
Human bocavirus (HBoV)
HiBiT tag
Infectious clone
Antiviral drug evaluation

ABSTRACT

Human bocavirus 1 (HBoV1; family: *Parvoviridae*) causes a wide spectrum of respiratory diseases in children and gastroenteritis in adults. A lack of sensitive cell lines and efficient animal models hinders research on HBoV, including the development of anti-HBoV drugs or vaccines. Although the construction of a wild-type HBoV1 infectious clone has been reported, generating HBoV1 infectious clone carrying foreign reporter genes with suitable insertion sites in its genome while retaining replicative ability remains challenging. Here, HBoV1 infectious clones harboring the 11-amino-acid HiBiT tag at five distinct insertion sites were constructed and evaluated. Only the recombinant HBoV1 carrying the HiBiT tag in the N-terminus of the NS1 protein (HBoV1-HiBiT$_{NS1}$) displayed comparable characteristics to wild-type HBoV1 as determined via the analysis of viral DNA copy number, NanoLuc activity, viral protein expression, and the formation of replication intermediates. Notably, the replication kinetics of HBoV1-HiBiT$_{NS1}$ could be examined by monitoring NanoLuc activity, which was noted to be correlated with the viral DNA level. Additionally, we successfully applied HiBiT-tagged HBoV1 for the evaluation of antiviral drug activity and identified ivermectin (EC50 = 2.27 μM) as a potent anti-HBoV1 replication drug. Overall, our study demonstrated that the HBoV1-HiBiT$_{NS1}$ reporter can serve as a convenient platform for screening candidate drugs targeting HBoV1 replication and may also be useful for investigating the life cycle of the virus.

INTRODUCTION

Human bocavirus 1 (HBoV1; genus: *Bocaparvovirus*, family: *Parvoviridae*) is an emerging human pathogenic respiratory virus that causes lower respiratory tract infections in young children worldwide (Christensen et al., 2019; Trapani et al., 2023). However, no specific clinically approved treatment for HBoV infection is currently available (Trapani et al., 2023).

HBoV1 is a nonenveloped, typical icosahedral, single-stranded DNA virus with a virion size of ~26 nm and a 5.5-kb genome flanked by inverted terminal repeats at both ends (Shao et al., 2021; Mohammadi, 2023). HBoV1 transcribes a single pre-mRNA from a promoter (P5) at the left end of the genome (nt 282), which is processed via alternative splicing and alternative polyadenylation, generating at least 12 mature mRNA transcripts (Shao et al., 2021). The HBoV1 genome comprises three open reading frames (ORF1, ORF2, and ORF3) that encode three structural proteins (VP1, VP2, and VP3) and six non-structural proteins (NS1, NS1-70, NS2, NS3, NS4, and NP1) (Shao et al., 2021; Colazo Salbetti et al., 2023; Mohammadi, 2023). VP1, VP2, and VP3 share a C-terminus and constitute the viral capsid in a ratio of 1:1:10 (Mohammadi, 2023). The capsid surface of the virus carries host determinants and is involved in many processes, including host tropism,

* Corresponding authors.
E-mail addresses: tang_jielin@gzlab.ac.cn (J. Tang), yang_qi@gzlab.ac.cn (Q. Yang).
[1] Jielin Tang and Sijie Chen contributed equally to this work.

https://doi.org/10.1016/j.virs.2025.03.009
Received 30 September 2024; Accepted 21 March 2025
Available online 25 March 2025

pathogenicity, assembly, and the immune response (Kailasan et al., 2016; Mietzsch et al., 2017). The HBoV1 nonstructural proteins NS1, NS2, NS3, and NS4 have reported molecular masses of ~100, ~66, ~69, and ~34 kDa, respectively (Deng et al., 2017), and share the C-terminus of the NS1 protein (aa 639 to 781). NP1 (219 aa), a protein unique to bocaparvoviruses, is localized to viral replication centers (Shen et al., 2016). HBoV1 NS proteins have been shown to help initiate and sustain the replication of the viral genome as well as mediate several important virus-host cell interactions (Shen et al., 2015; Deng et al., 2017). Meanwhile, NS1 and NP1 are relatively conserved proteins, and both can serve as targets for HBoV detection (Shao et al., 2021; Trapani et al., 2023).

In 2012, a reverse genetics system for HBoV1 was established, in which it was shown that HEK293T or HEK293 cells can replicate the viral duplex genome, producing progeny virions at a high titer by transfecting HBoV1 infectious clone (Huang et al., 2012). Reporter genes in viruses can be valuable tools for studying viral pathogenesis and the screening of antiviral drugs. However, to date, no recombinant parvovirus, including HBoV, harboring a reporter gene has been reported. The genomes of parvoviruses contain overlapping ORFs and generate multiple transcripts (Shan et al., 2010; Shen et al., 2015), which makes it difficult to find a suitable insertion site for a foreign gene without impairing the viral life cycle. Moreover, there is a strict limit on the genome size that can be efficiently packaged into virus capsids (Sumiyadorj et al., 2022; Yu et al., 2024). This restricted packaging capacity of small DNA or RNA viruses precludes the recombinant viruses carrying larger genes (Eyre et al., 2017; Tamura et al., 2019; Sumiyadorj et al., 2022; Yu et al., 2024).

HiBiT is an 11-aa split-reporter tag derived from NanoLuc binary technology, known as NanoBiT. Complementation with its counterpart LgBiT results in a highly active NanoBiT luciferase enzyme (Dixon et al., 2016). Consequently, proteins tagged with HiBiT can be easily detected and their activity measured using bioluminescence via the Nano-Glo assay system (Zhang et al., 2023). HiBiT has been successfully applied in several recombinant viruses, including influenza A virus (Zhang et al., 2023), hepatitis E virus (Nagashima et al., 2023), enterovirus A71 (Yu et al., 2024), coxsackievirus (Yu et al., 2024), and *Flaviviridae* viruses such as JEV, HCV, and CSFV (Tamura et al., 2018, 2019). These studies suggest that recombinant viruses carrying the HiBiT tag are effective tools for antiviral drug screening and viral spatiotemporal dynamic monitoring. Moreover, they have collectively demonstrated the suitability of employing the HiBiT tag for constructing infectious clones, given its small size.

Here, we succeeded in constructing HBoV1 infectious clones carrying the HiBiT tag at five distinct insertion sites. Subsequent investigation showed that only the clone harboring the HiBiT tag fused to the N-terminus of the NS1 protein (HBoV1-HiBiT$_{NS1}$) exhibited growth characteristics comparable to those of the wild-type virus *in vitro*. Moreover, we successfully applied HBoV1-HiBiT$_{NS1}$ for the evaluation of the antiviral activity of several drugs and identified ivermectin (EC50 = 2.274 μM) as a potent inhibitor of HBoV1 replication. This demonstrated the promising potential of HBoV1-HiBiT$_{NS1}$ infectious clone for use in high-throughput drug screening.

RESULTS

Insertion sites for the HiBiT coding sequence in the HBoV1 genome

Given that the HBoV1 genome contains overlapping ORFs, we first considered fused the HiBiT sequence at the N-terminus common to NS1, NS1-70, and NS2; the C-terminus common to NS1-70, NS2, NS3, and NS4; and the C-terminus common to all the structural proteins (Fig. 1A). Additionally, we contemplated displaying HiBiT on the surface of viral particles. Thus, analysis of the solvent-accessible surface area of each amino acid of the VP3 protein (score > 20) indicated that four amino acid residues—aas 32, 143, 206, and 460—have the potential to be exposed on the particle surface (Supplementary Fig. S1A). Accordingly, we further selected the coil and turn sites (Supplementary Fig. S1B), which were benefit for foreigner gene insertion, and the less conservative residues of VP3 (aas 206 and 460; Supplementary Fig. S1C) as candidate sites for HiBiT insertion. Analysis of the solvent-accessible surface area using Swiss-PDBViewer 4.0 software suggested that when inserted at each of the 5 selected sites, the HiBiT tag had the potential to be displayed on the surface of the respective proteins (Fig. 1B). Subsequently, recombinant cDNA clones of HBoV1, namely, pHBoV1-HiBiT$_{NS1}$, pHBoV1-HiBiT$_{NS1\text{-}70}$, pHBoV1-HiBiT$_{VP3}$, HBoV1-HiBiT$_{VP3\text{-}206}$, and HBoV1-HiBiT$_{VP3\text{-}460}$, were constructed by inserting the HiBiT (VSGWRLFKKIS) and linker (GSSG) sequences at the five selected sites (Fig. 1A, black arrows), and the generated clones were confirmed by sequencing. Additionally, a stable HEK293T-LgBiT cell line was generated and was determined to function efficiently, as evaluated by the detection of LgBiT protein expression (Supplementary Fig. S2A) and NanoLuc activity (Supplementary Fig. S2B).

Analysis of the replication capacity of HBoV1 recombinant infectious clones

We next analyzed whether the constructed recombinant cDNA clones had replicative ability with pHBoV1-WH serving as the control. Luciferase activity and HBoV1 DNA, mRNA, and protein levels were determined in HEK293T-LgBiT cells expressing the respective recombinant HBoV1 clones at 72 h post-transfection. Bioluminescence analysis showed that only the HEK293T-LgBiT cells expressing pHBoV1-HiBiT$_{NS1}$ were positive for luciferase activity (Fig. 2A), indicating that pHBoV1-HiBiT$_{NS1}$ has the potential to replicate in HEK293T cells. This was further confirmed via the quantification of the intracellular levels of viral DNA (Fig. 2B), viral mRNA (Supplementary Fig. S3A–E), viral proteins (NS1, NP1, and VPs), and the HiBiT tag (Fig. 2C, lane 3). Notably, luciferase activity, HBoV1 DNA levels, and NSs protein expression were markedly inhibited in cells transfected with the clone carrying HiBiT in the C-terminus of NS1-70 (Fig. 2A–C, lane 4), suggesting that the insertion of a foreign gene at this site may disrupt both viral replication and viral protein expression. Meanwhile, in the infectious clones in which the HiBiT tag was inserted into the VP3 protein (Fig. 2B), HBoV1 retained approximately 50% of its replicative ability, whereas a significant decrease was observed in luciferase activity (Fig. 2A) and the expression levels of structural proteins and the HiBiT peptide tag (Fig. 2C, lanes 5–7); however, there was no marked change in the levels of viral mRNA transcripts in these five infectious clones (Supplementary Fig. S3A–E), indicating that the attachment of the HiBiT tag onto the VP3 protein may affect the expression of viral structural proteins and HiBiT tag, thereby inhibiting viral replication. Additionally, the decline in the expression of viral proteins following the transfection of HBoV1-HiBiT$_{NS1\text{-}70}$, HBoV1-HiBiT$_{VP3}$, HBoV1-HiBiT$_{VP3\text{-}206}$, and HBoV1-HiBiT$_{VP3\text{-}460}$ could not be reversed with the addition of inhibitors of protein degradation (Supplementary Fig. S3F–H), suggesting that viral protein expression may be regulated by other post-transcriptional mechanisms.

The viral replication intermediates of the five clones carrying the HiBiT tag were further evaluated by Southern blotting. Newly synthesized DNA, namely, the DpnI digestion-resistant double replicative form (dRF) and monomer replicative form (mRF), were detected in cells transfected with the HBoV1-HiBiT$_{NS1}$ clone, which showed a replicative capacity comparable to that of the WT infectious clone (Fig. 2D). Moreover, the insertion of HiBiT in the C-terminal of NS1-70 indeed impaired the replication intermediates formation, and the replication capacity of other infectious clones including (HBoV1-HiBiT$_{NS1}$, HBoV1-HiBiT$_{VP3}$, HBoV1-HiBiT$_{VP3\text{-}206}$, and HBoV1-HiBiT$_{VP3\text{-}460}$) was not significantly affected (Fig. 2D).

We also constructed HBoV1 recombinants incorporating a GFP gene in the N-terminus of NS1 (HBoV1-GFP$_{NS1}$). After transfecting in HEK293T cells, we indeed observed GFP fluorescence (Supplementary Fig. S4A), which was further supported by detection of NSs-GFP fusion protein (Supplementary Fig. S4B); however, the expression of other

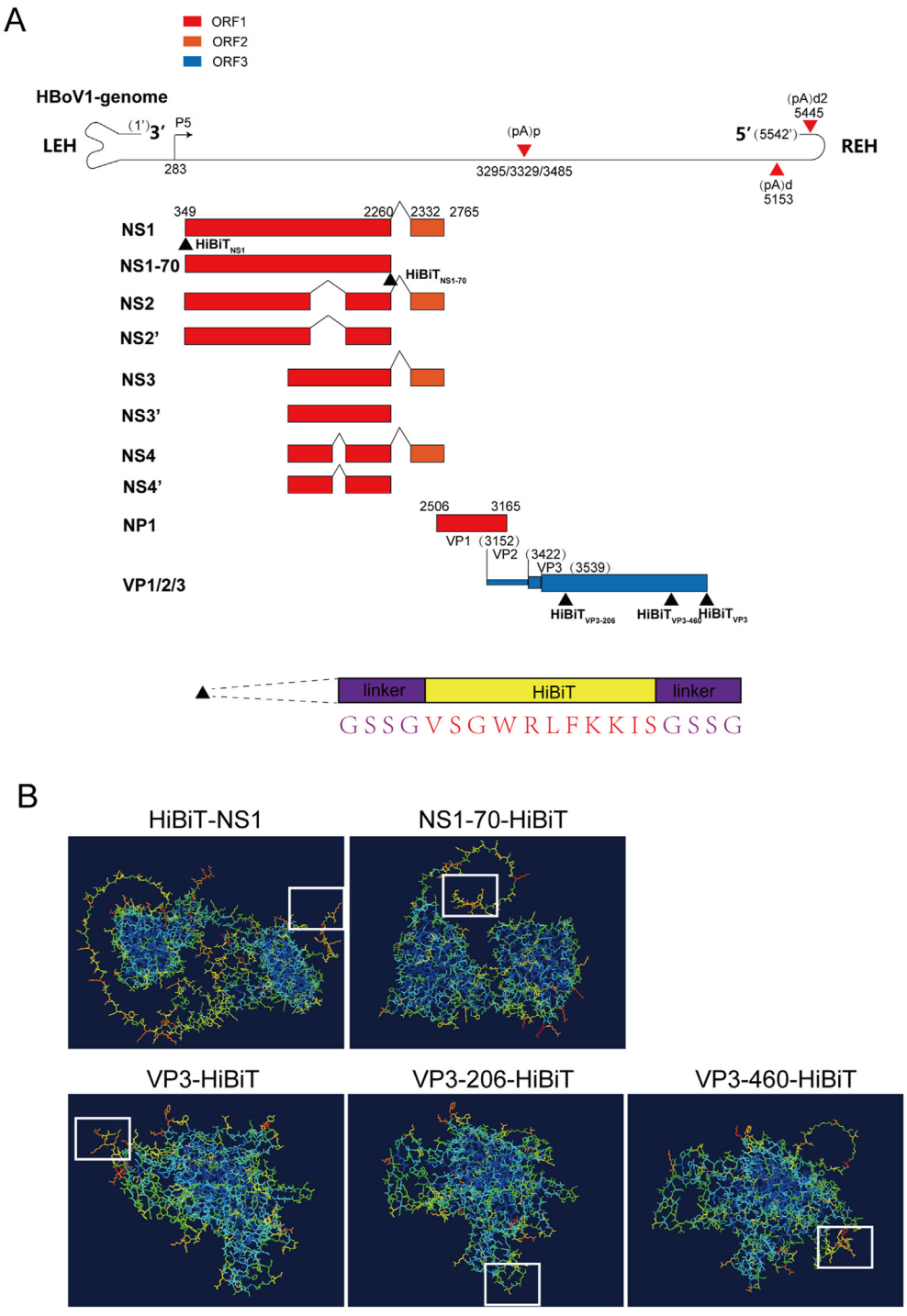

Fig. 1. Insertion sites for the HiBiT coding sequence in the HBoV1 genome. **A** Diagram showing the pHBoV1 genome structure. Black arrows and numbers indicate HiBiT tag insertion sites. The HiBiT tag (yellow) and GSSG linker (purple) sequences are indicated. **B** Prediction of the accessibility of NS1, NS1-70, and VP3 after the insertion of the HiBiT tag using Alphafold2. Accessibility (from strong to weak): red > yellow > green > blue.

viral proteins (NP1 and VPs) and replication intermediates was impaired (Supplementary Fig. S4B and C). Meanwhile, compared with wild-type HBoV1, the HBoV1-GFP$_{NS1}$ DNA copy number was significantly reduced (Supplementary Fig. S4D), suggesting that the length of the inserted foreign gene is also a critical factor for HBoV1 replication.

Taken together, these findings indicated that the N-terminus of NS1 is the optimal insertion site for the HiBiT tag to create HBoV recombinant infectious clones.

Characterization of recombinant HBoV1 carrying the HiBiT tag in the NS1 protein

To characterize HBoV1-HiBiT$_{NS1}$, we first investigated its subcellular localization by immunofluorescence using antibodies targeting either NS1 or HiBiT. Immunofluorescence analysis showed that NS1 and HiBiT colocalized in cells transfected with HBoV1-HiBiT$_{NS1}$ (Fig. 3A). Then, the benzonase resistant DNA successfully detected in the supernatants of HEK293T cells after transfection with pHBoV1-HiBiT$_{NS1}$ verified that the

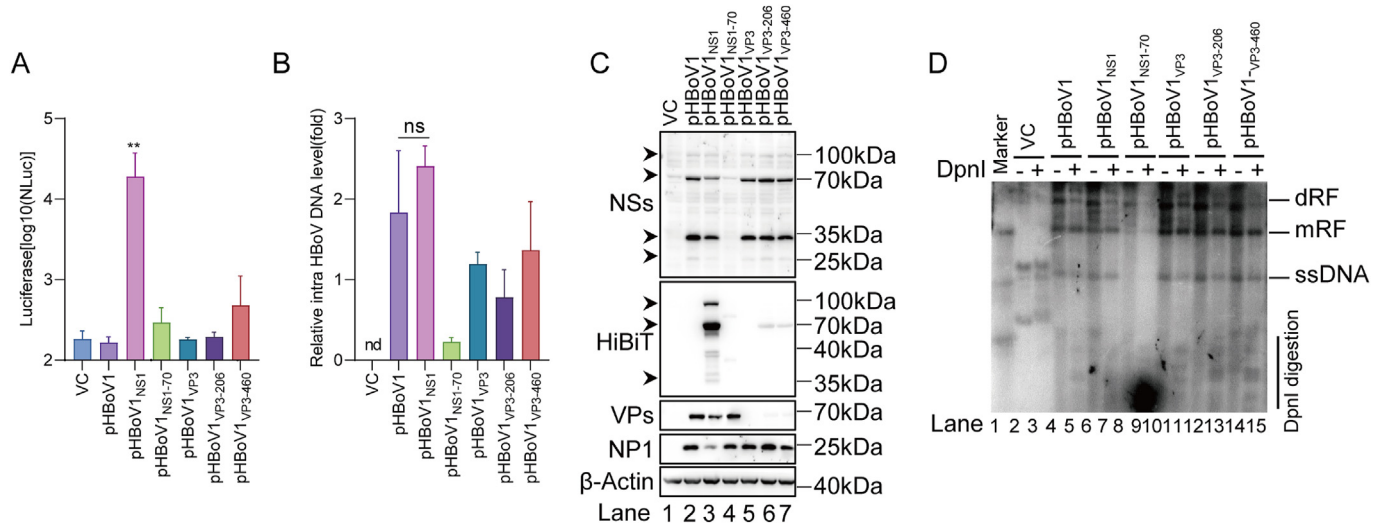

Fig. 2. Analysis of the replication capacity of the HBoV1 recombinant clones. **A** HEK293T cells overexpressing LgBiT were separately transfected with different pHBoV1-HiBiT plasmids (pHBoV1, pHBoV1-HiBiT$_{NS1}$, pHBoV1-HiBiT$_{NS1\text{-}70}$, pHBoV1-HiBiT$_{VP3}$, pHBoV1-HiBiT$_{VP3\text{-}206}$, or pHBoV1-HiBiT$_{VP3\text{-}460}$); after 72 h, HiBiT-dependent luciferase activity was measured. **B** HEK293T cells were separately transfected with different pHBoV1-HiBiT plasmids; after 72 h, the intracellular DNA replication level was quantified by qPCR [compared to wild type (WT)]. **C** HEK293T cells were separately transfected with different pHBoV1-HiBiT plasmids; after 48 h, the protein levels of NS1, HiBiT, VPs, and NP1 were quantified by western blotting. **D** HEK293T cells were transfected with pHBoV1, pHBoV1-HiBiT$_{NS1}$, pHBoV1-HiBiT$_{NS1\text{-}70}$, pHBoV1-HiBiT$_{VP3}$, pHBoV1-HiBiT$_{VP3\text{-}206}$, or pHBoV1-HiBiT$_{VP3\text{-}460}$; subsequently, Hirt-extracted DNA was digested with the DpnI restriction endonuclease for 12 h and separated using 1.2% agarose gel electrophoresis. dRF (double replicative form) DNA and mRF (monomer replicative form) DNA, which was resistant to digestion by DpnI, was detected in the transfected cells by Southern blotting. Data are representative of three independent experiments. The graphs show means ± SD; n = 3. **, $P < 0.01$; nd, undetermined; ns, not significant.

recombinant HBoV1-HiBiT$_{NS1}$ virus could be released (Fig. 3B). To further evaluate HBoV1 replication and the specificity of luciferase activity in HBoV1-HiBiT$_{NS1}$ clones, wild-type HBoV1 and recombinant HBoV1-HiBiT$_{NS1}$ clones were transfected into HEK293T-LgBiT cells, and intracellular HBoV1 DNA contents, luciferase activity, and viral protein expression were determined at different times points (Fig. 3C–E). The results showed that the growth kinetics of recombinant HBoV1-HiBiT$_{NS1}$ clones were similar to those of wild-type HBoV1. Additionally, the increase in intracellular HBoV1 DNA levels was comparable between the HBoV1-HiBiT$_{NS1}$ and HBoV1-WT. Meanwhile, luciferase activity in cells transfected with HBoV1-HiBiT$_{NS1}$, but not with the wild-type virus, increased in line with the increase in intracellular viral DNA, reflecting virus replication (Fig. 3C and D). Moreover, the expression trend of viral proteins in HBoV1-HiBiT$_{NS1}$-transfected cells was similar to that in cells harboring wild-type HBoV1, peaking at 48 h post-transfection, and the anti-HiBiT antibody only detected HiBiT-NS1 in cells transfected with the HBoV1-HiBiT$_{NS1}$ clone (Fig. 3E). Collectively, these data further supported that the recombinant HBoV1-HBiT$_{NS1}$ clone exhibits a comparable replication capacity to that of wild-type HBoV1.

To further compare the features of HiBiT-tagged and wild-type viruses, we next amplified and purified the virus in HEK293T cells. The purified viruses were subsequently negatively stained and subjected to transmission electron microscopy. The results showed that the HBoV1-HiBiT$_{NS1}$ virions were identical to the wild-type particles in both morphology and size (spherical, ~26 nm in diameter) (Fig. 3F). Immunoelectron microscopy using immunogold labeling revealed that the anti-VP antibody recognized both wild-type HBoV1 and the HBoV1-HiBiT$_{NS1}$ recombinant (Fig. 3G). These data indicated that the insertion of the HiBiT sequence in the N-terminus of NS1 does not affect HBoV1 particle formation. Moreover, the infectivity of HBoV1-HiBiT$_{NS1}$ recombinant strain in MA104 cells (a permissive cell line for HBoV1 infection (Tang et al., 2025)) has been detected. The results showed that the recombinant HBoV1-HiBiT$_{NS1}$ intracellular virus DNA copies could quantified in MA104 cells, which were slightly better than the HBoV1 strain (Fig. 3H).

In summary, these results demonstrated that the insertion of the small HiBiT sequence has a minimal impact on HBoV1 replication and assembly.

Evaluation of antiviral drugs using recombinant HBoV1-HiBiT$_{NS1}$

There is currently no clinically approved, specific treatment for HBoV1 infection. Accordingly, we next used HBoV1-HiBiT$_{NS1}$ to evaluate the anti-HBoV1 activity of eight compounds (cidofovir, favipiravir, ivermectin, nevirapine, remdesivir, ribavirin, sofosbuvir, zidovudine). Among these, cidofovir and ivermectin have been reported to inhibit the replication of B19V, a parvovirus, while the others are broad-spectrum inhibitors of viral replication that target RNA-dependent RNA polymerase (RdRp) or RNA/DNA-dependent DNA polymerase. HEK293T-LgBiT cells were pre-incubated with these compounds for 2 h and then transfected with HBoV1-HiBiT$_{NS1}$. At 72 h post-transfection, the Nano-Glo luciferase assay was performed and the luminescent signals were measured. Ivermectin (10 μM) treatment significantly inhibited HBoV1 replication, and cidofovir (200 μM), nevirapine (50 μM), and ribavirin (50 μM) displayed ~50% inhibition efficiency against luciferase activity (Fig. 4A). Because ivermectin exhibited the best anti-HBoV1 effect, we next sought to determine its EC50 value. We found that ivermectin inhibited luciferase activity in a dose-dependent manner in HEK293T-LgBiT cells transfected with HBoV1-HiBiT$_{NS1}$, with an EC50 value of 2.274 μM (Fig. 4B). The selectivity index of ivermectin exceeded 4.123 (Fig. 4B), indicative of its safety at the cellular level. Ivermectin also dose-dependently decreased intracellular HBoV1 DNA levels, further confirming its potent inhibitory effect on HBoV1 replication (Fig. 4C) and suggesting that HiBiT-tagged recombinant HBoV1 is a useful tool for the screening of antiviral agents. Collectively, these results also indicated the feasibility of using the pHBoV1-HiBiT$_{NS1}$ to investigate virus replication.

DISCUSSION

HBoV1 is an emerging pathogen, with an increasing number of infections being reported worldwide. To date, there is no specific clinically approved treatment for bocavirus infection. Recombinant viruses carrying reporter genes have played a crucial role in simplifying the intracellular dynamic monitoring of viruses in both basic and applied studies. Here, we sought to identify appropriate sites for the insertion of a small HiBiT tag to generate HBoV1-HiBiT recombinants suitable for *in vitro*

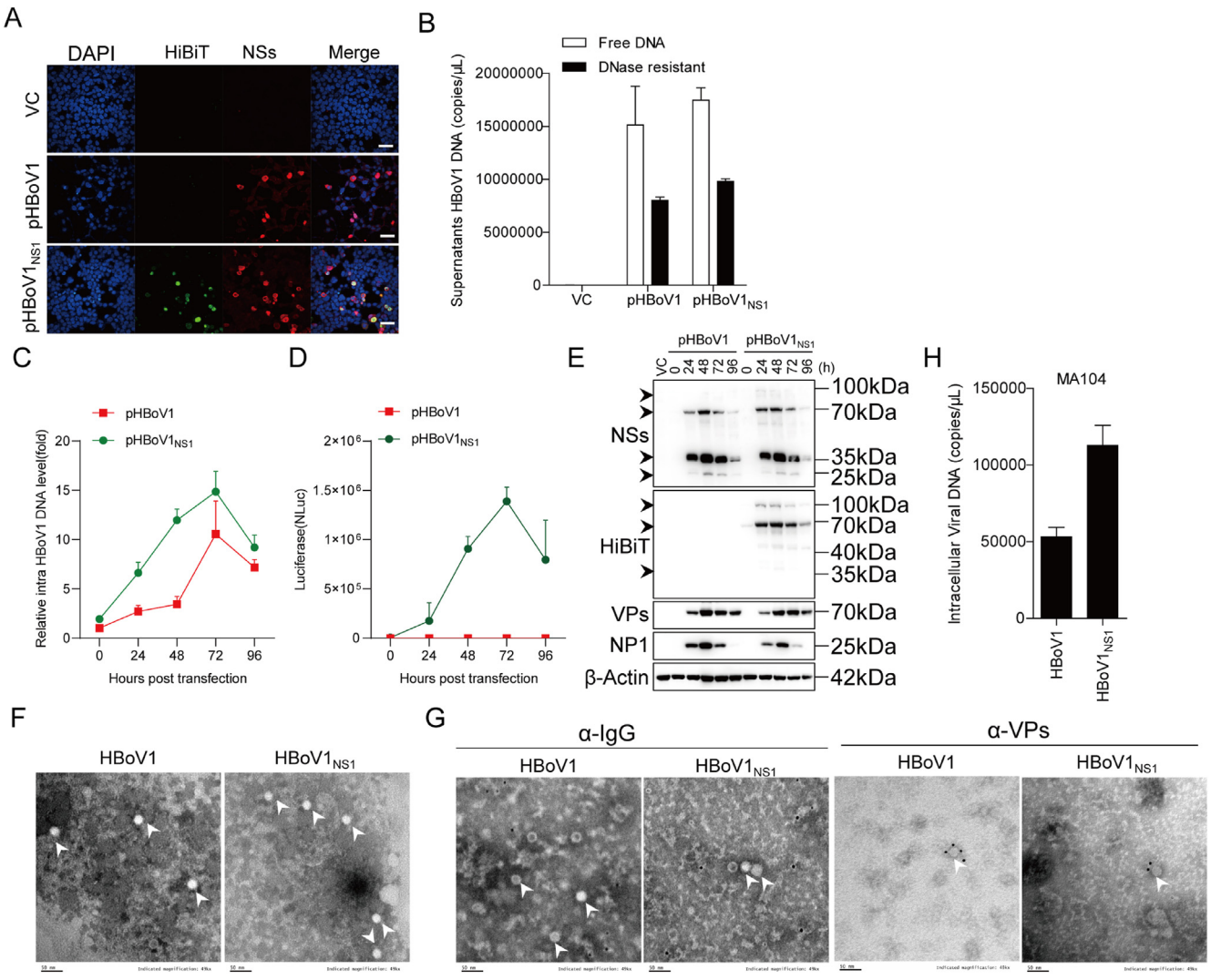

Fig. 3. Characterization of recombinant HBoV1 carrying the HiBiT tag in the NS1 protein. **A** HEK293T cells were transfected with pHBoV1 or pHBoV1-HiBiT$_{NS1}$ for 72 h, probed with the DNA-binding dye DAPI (blue), anti-HiBiT antibody (green) and anti-NS1 antibody (red) in an immunofluorescence analysis, and then subjected to confocal microscopy. Scale bars, 10 μm. **B** HEK293T cells were separately transfected with vector, pHBoV1, or pHBoV1-HiBiT$_{NS1}$ plasmids; after 48 h, the supernatant was collected with benzonase digestion or not for 30 min, then the benzonase resistant or free DNA in the supernatants was quantified by qPCR. **C–E** HEK293T cells were transfected with pHBoV1 or pHBoV1-HiBiT$_{NS1}$ and the intracellular DNA copy number **(C)**; HiBiT activity **(D)**; and NS1, VPs, NP1, and HiBiT protein levels **(E)** were quantified at the indicated time points. **F** HEK293T cells were transfected with pHBoV1 or pHBoV1-HiBiT$_{NS1}$ for 72 h, after which HBoV1 and HBoV1-HiBiT$_{NS1}$ virions were subjected to negative-stain scanning electron microscopy. Scale bars, 50 nm. **G** Transmission electron microscopy of immunogold labeling in HBoV1 and HBoV1-HiBiT$_{NS1}$ virions. Anti-VP antibodies were used as the primary antibodies. Goat anti-rabbit IgG (negative control) conjugated with 6-nm colloidal gold served as the secondary antibody. Scale bars, 50 nm. **H** MA104 cells were infected with 3000 vge/cell of HBoV1 or HBoV1-HiBiT$_{NS1}$ for 96 h. The intracellular HBoV1 DNA copies were quantified.

investigation. We constructed five HBoV1 infectious clones carrying the HiBiT tag in distinct insertion sites and found that the fusion of the HiBiT tag to the N-terminus of the NS1 protein exerted only minimal effects on HBoV1 replication. The recombinant HBoV1-HBiT$_{NS1}$ clone displayed a comparable replication capacity with that of wild-type HBoV1, and the insertion of the HiBiT sequence in the N-terminus of NS1 did not influence HBoV1 particle formation. Furthermore, we demonstrated the utility of HBoV1-HiBiT$_{NS1}$ for the *in vitro* screening of antivirals targeting HBoV1 replication. Among several drugs tested, we found that ivermectin has a potent inhibitory effect on HBoV1 replication.

Various reporter proteins, such as GFP, NanoLuc luciferase, and firefly luciferase, have been incorporated into many viral particles to elucidate viral dynamics and develop antiviral reagents. However, the application of small RNA or DNA viruses carrying a large foreign gene remains limited, given the restricted ability of these viruses to accommodate such insertions in their genomes. For example, a recombinant DENV carrying the full-length NanoLuc luciferase in NS1 displayed impaired replication (Eyre et al., 2017), while viable progeny could not be obtained from recombinant enteroviruses carrying NanoLuc luciferase (Yu et al., 2024). In our study, we also generated a recombinant HBoV1 infectious clone harboring GFP but found that its replication ability was markedly attenuated. This negative effect on virus replication may have been due to the size of the foreign gene incorporated into the viral genome and/or the dampening effect of the insertion site on the function of viral proteins. Inserting HiBiT (11 aa) in infectious clones might solve the problem of foreign gene size. In this study, different HiBiT insertion sites in HBoV1 infectious clones were evaluated, but only the recombinant clone carrying the HiBiT tag in the N-terminus of the NS1 protein exhibited levels of replication comparable to those of the wild-type virus. Furthermore, except for HBoV1-HiBiT$_{NS1\text{-}70}$, the replication capacity of the other three recombinant viruses was attenuated, as was their luciferase activity. This may have been due to a reduction in the expression

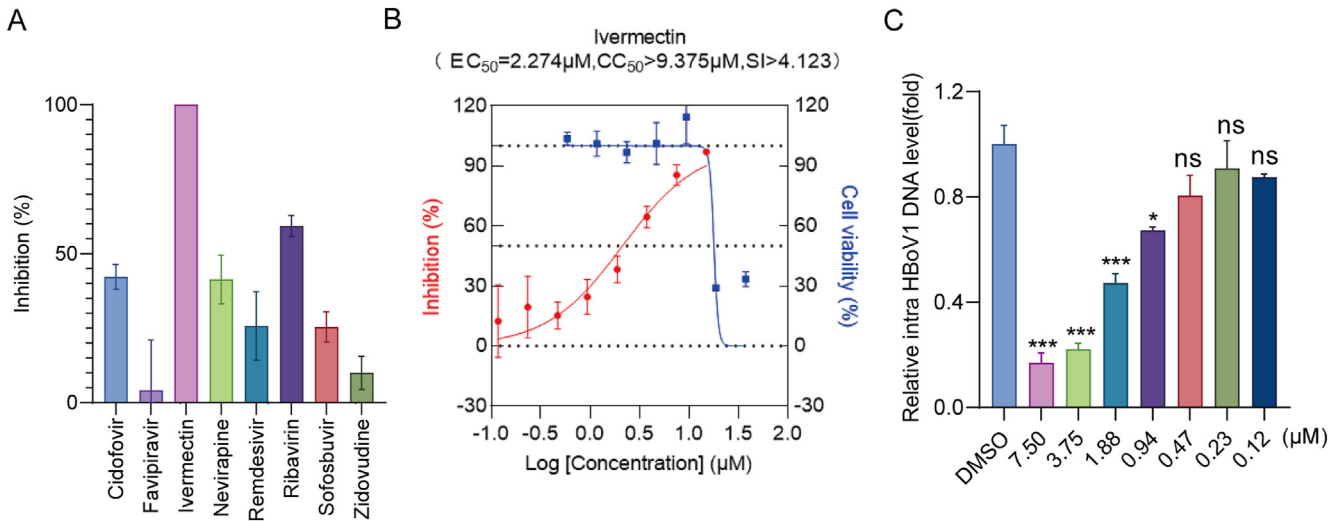

Fig. 4. Evaluation of antiviral drugs using recombinant HBoV1-HiBiT$_{NS1}$. **A** HEK293T cells were transfected with pHBoV1-HiBiT$_{NS1}$ in the presence of cidofovir (200 μM), favipiravir (50 μM), ivermectin (10 μM), nevirapine (50 μM), remdesivir (10 μM), ribavirin (50 μM), sofosbuvir (50 μM), or zidovudin (50 μM). At 72 h post-transfection, the Nano-Glo luciferase assay was performed. **B, C** HEK293T cells were transfected with pHBoV1-HiBiT$_{NS1}$ in the presence of increasing (2-fold) concentrations of ivermectin. At 72 h post-transfection, luciferase activity was measured using the Nano-Glo luciferase assay **(B)**, while the intracellular DNA copy number was quantified by qPCR **(C)**. The EC50 and CC50 values were determined by fitting the dose-response curves with four-parameter logistic regression in GraphPad Prism. *, $P < 0.05$, ***, $P < 0.001$; ns, not significant.

levels of viral proteins and the HiBiT tag or, alternatively, that the inserted HiBiT tag was not localized on the surface of the fusion protein; however, these possibilities require confirmation. Additionally, it has been reported that, in the H2N3 virus, the direct addition of an extra tag to either the N- or C-terminus of other viral proteins besides NS1 and NEP can also disrupt the packaging signals needed for progeny virion assembly (Heaton et al., 2013; Tran et al., 2013). Thus, the insertion of the HiBiT tag at the C-terminus of the structural protein VP3 might have impaired the expression of all three VPs and led to a reduction in virion assembly efficiency. In our study, the insertion of HiBiT in the C-terminus of NS1–70 almost completely abolished HBoV1 replication ability, luciferase activity, and viral protein expression; this may have resulted from the destroy of the transcription of NS proteins or the function of NS1, a multifunctional protein important for virus replication (Shen et al., 2015; Zhu et al., 2019). Although the optimal internal sites for the insertion of HiBiT require further rational design and evaluation; by combining rational design and evaluation, it may also be possible to determine suitable sites for the insertion of foreign peptides into other *Parvoviridae* viruses.

HBoV1 only infects differentiated, polarized, primary human airway epithelial (HAE) cells and tends to replicate at both the apical and basal surfaces of HAE cells cultured at an air-liquid interface (ALI) (Mohammadi, 2023). The HEK293T (kidney epithelial) and Caco-2 (colon epithelial) cell lines have been reported as being partially permissive for HBoV-1 infection (Dijkman et al., 2009; Huang et al., 2012; Ghietto et al., 2017). HEK293T cells produce high titers of infectious progeny virions upon transfection, indicating that virus replication is highly efficient in the cells (Huang et al., 2012). Theoretically, utilizing the HiBiT tag for the screening of drugs targeting HBoV1 replication in HEK293T cells is feasible. In our study, we found that the HBoV1-HiBiT$_{NS1}$ infectious clone exhibits a replicative capacity similar to that of wild-type HBoV1. In the HBoV1-HiBiT$_{NS1}$ clone, luciferase activity was positively correlated with the kinetics of intracellular DNA copy number, indicating that HBoV1 replication can be dynamically monitored through the measurement of luciferase activity. Recently, it has reported that T84 (originate from the lung metastasis of a colorectal tumor) monolayer cell cultures or T84 air-liquid interface cultures supports productive HBoV replication (Schildgen et al., 2018; Soldwedel et al., 2024). Nevertheless, although we evaluated the replication capacity and virus particle formation of HBoV1-HiBiT$_{NS1}$, and its infectivity in MA104 cells (a permissive cell line for HBoV1 infection) (Tang et al., 2025), and the infectivity of this recombinant virus needs further assessment in HAE-ALI culture system. Interestingly, in our study, the purified HBoV1-HiBiT$_{NS1}$ virus was immunostained with an anti-HiBiT antibody, followed by detection using a colloidal gold-conjugated antibody; this hinted that the HiBiT tag might have integrated on the surface of viral particles as a component of this purified HBoV1-HiBiT virus. Recent research showed that the membrane-coating of B19V virions facilitates virus release (Ishida et al., 2023). The complete HBoV1 particle has not yet been resolved, and the composition of its capsid is not clear. NS1 may function as a component of the viral particle during virus maturation or release. Further studies are needed to determine the role of NS1 in HBoV1 particle formation.

In this study, we demonstrated the utility of HBoV1-HiBiT$_{NS1}$ for *in vitro* antiviral screening. Specifically, we identified ivermectin as a potent inhibitor of HBoV1 replication and found that cidofovir also exerts an inhibitory effect on the replication of this virus. Both drugs have been reported to inhibit the replication of B19V, suggestive of their therapeutic potential against B19V-induced disease (Bonvicini et al., 2015, 2016; Alvisi et al., 2023). Given that B19V is a member of the *Parvoviridae* family, this indicates that these drugs may also be effective against HBoV1. It is necessary to further evaluate the antiviral activity of these drugs in an infection system. Additionally, parvoviruses typically enter cells via receptor-mediated endocytosis, which involves a virion binding to specific receptors on the host cell surface, followed by internalization of the virus into the host cell (Mohammadi, 2023). HEK293T cells did not support HBoV1 entry, most likely due to a lack of receptors for the virus. Thus, it may be worthwhile to find a receptor for HBoV1 entry by using this recombinant virus to further investigation.

CONCLUSIONS

In summary, we constructed a recombinant HBoV1 infectious clone possessing a small luciferase subunit in the N-terminus of the NS1 protein and found that it has a replication capacity comparable to that of wild-type HBoV1. Moreover, our study identified the usefulness of this recombinant virus for the screening of antiviral agents and for the investigation of viral dynamics *in vitro*, which will be of benefit to antiviral and vaccine development.

MATERIALS AND METHODS

Reagents and antibodies

The small-molecule compounds cidofovir (#HY-17438), favipiravir (#HY-14768), ivermectin (#HY-15310), nevirapine (#HY-10570), remdesivir (#HY-104077), ribavirin (#HY-B0434), sofosbuvir (#HY-15005), and zidovudine (#HY-17413) were purchased from MCE. Hoechst (#H1398) and benzonase nuclease (#88701) were sourced from Invitrogen. Antibodies against NS, NP1, and VP proteins (for immunofluorescence or western blotting) were custom-produced by Sino Biological. Monoclonal antibodies targeting HiBiT (#N7200) and LgBiT (#N7100) were obtained from Promega. The monoclonal antibody against β-actin (#66009–1) was purchased from Proteintech.

Cell culture

All the cells were cultured at 37 °C in a humidified atmosphere with 5% CO_2. HEK293T cells were obtained from American Type Culture Collection and cultured in Dulbecco's modified Eagle's medium (Invitrogen) supplemented with 2 mM L-glutamine, nonessential amino acids, 10% fetal bovine serum (FBS) (Invitrogen), and 1% penicillin–streptomycin (Life Technologies).

Plasmids

The recombinant infectious clone pHBoV-1-WH was provided by H. Z. Wang and W. X. Guan (Wuhan Institute of Virology). In-Fusion cloning was used to construct the plasmids pHBoV1-HiBiT$_{NS1}$, pHBoV1-HiBiT$_{NS1\text{-}70}$, pHBoV1-HiBiT$_{VP3}$, pHBoV1-HiBiT$_{VP3\text{-}206}$, and pHBoV1-HiBiT$_{VP3\text{-}460}$. Taking the construction of pHBoV1-HiBiT$_{NS1\text{-}70}$ as an example, pHBoV1-WH was first digested with MscI and AlarI. The HiBiT segment was amplified using primers (MscI-NS1-70-Hibit-F and NS1-70-Hibit-AlarI-R) designed to add an overlap of more than 20 bases relative to the template. Using the ClonExpress Ultra One Step Cloning Kit (Vazyme), the fragments fused HiBiT tag were then cloned into the vector of pHBoV1-WH after restriction enzyme digestion. The sequences of the primers used are listed in Supplementary Table S1.

Quantitative reverse transcription-polymerase chain reaction (qRT-PCR)

For the quantification of the transcript levels of the different HBoV1 genes, total RNA was extracted from cells using TRIzol reagent (Invitrogen) according to the manufacturer's instructions. One-step real-time qRT-PCR was conducted using the HiScript II One Step qRT-PCR SYBR Green Kit (Vazyme). β-Actin was used for normalization. Relative expression was calculated using the $2^{-\Delta\Delta CT}$ method. The primer sequences are provided in Supplementary Table S2.

Quantitative polymerase chain reaction PCR (qPCR)

Viral genomes were extracted from intracellular virions using the TIANamp Virus DNA/RNA Fast Kit (TIANGEN Biotech) according to the manufacturer's instructions. Viral DNA copy number was quantified by qPCR using the Taq Pro HS Universal Probe Master Mix (Vazyme). Absolute quantification was conducted using a standard curve. The primer sequences are provided in Supplementary Table S2.

Luciferase activity assay

For HiBiT activity evaluation, HEK293T-LgBiT cells were transfected with pHBoV1 or pHBoV1-HiBiT$_{NS1}$. After 72 h of transfection, luciferase activity was measured using a Nano-Glo HiBiT lytic detection system (Promega) according to the protocol provided by the manufacturer.

Western blotting

Western blotting was performed as previously described (Tang et al., 2023). Briefly, cells were lysed in lysis buffer for 30 min at 4 °C and centrifuged at 12,000 ×*g* for 10 min at 4 °C. After quantification, the proteins were separated using 10% SDS-PAGE, electro-transferred to nitrocellulose filter membranes (Millipore), blocked for 1 h with 5% nonfat milk, and incubated with the appropriate antibodies. The immune complexes were visualized using horseradish peroxidase-conjugated secondary antibodies (Jackson ImmunoResearch) and WesternBright Sirius HRP substrate (Advansta Inc.).

Southern blotting

HBoV-1 replicative forms form DNA were detected by Southern blotting as previously described (Qiu et al., 2006). Cells were collected, washed twice with PBS, lysed with TE buffer (10:10) (10 mM Tris-HCl, pH 7.5, and 10 mM EDTA) and 10% SDS for 30 min, subjected to phenol–chloroform-based Hirt DNA extraction, and digested or not with DpnI restriction endonuclease. After separation using 1.1% agarose gel electrophoresis, Southern blotting was performed using the HBoV1 dsDNA genome as the probe.

Transfection for HBoV1 or HBoV1-HiBiT$_{NS1}$ production and subsequent purification

HEK293T cells were seeded on 200-mm plates and transfected with pHBoV1-WH or pHBoV1-HiBiT$_{NS1}$ (50 μg) using Polyethylenimine Max transfection reagent (Mw 40,000) (Polysciences, Inc.) for 72 h. For the purification of intracellular virions, the cells were collected with PBS (pH 7.4), lysed by three rounds of freezing (−196 °C) and thawing (37 °C), and treated with benzonase nuclease (50 U/mL) for 1.5 h at 37 °C. The cell lysate was then centrifuged at 10,000 ×*g* for 30 min at 4 °C and the virions in the supernatant were further purified using a 20% (*w/v*) sucrose cushion in PBS and ultracentrifugation at 100,000 ×*g* for 2 h at 4 °C. The pellet was resuspended in PBS. Viral DNA was extracted using the TIANamp Virus DNA/RNA Fast Kit (TIANGEN) and the viral DNA copy number was quantified using qPCR.

Immunoelectron microscopy

HBoV1 and HBoV1-HiBiT$_{NS1}$ virions were purified as described above. For electron microscopy, 10 μL of each sample was placed on the grid for 1 min, after which excess sample was removed by touching the edge of the grid with filter paper. For negative staining, the samples were incubated with 10 μL of 2% phosphotungstic acid (pH 7.0) for 40 s. Excess liquid was absorbed with filter paper and the grids were then allowed to dry naturally. Immunogold labeling was performed as previously described (Nagashima et al., 2017). Anti-VP or anti-HiBiT monoclonal antibodies were used as the primary antibodies. Goat anti-mouse or goat anti-rabbit IgG conjugated with 6-nm colloidal gold served as the secondary antibody (Jackson ImmunoResearch). Virions were observed using a transmission electron microscope (Tecnai G2 Spirit) at an acceleration voltage of 120 kV.

Determination of the antiviral activity of pHBoV1-HiBiT$_{NS1}$

For the determination of the antiviral activity of pHBoV1-HiBiT$_{NS1}$, HEK293T-LgBiT cells were seeded in 96-well plates and transfected with pHBoV1-HiBiT$_{NS1}$ (100 ng/well) in the presence of increasing concentrations of ivermectin. At 72 h post-transfection, a Nano-Glo luciferase assay was performed and the luminescent signals served as a readout of virus replication. The antiviral activity of the compound at 72 h post-infection was expressed as the IC50, that is, the concentration of ivermectin required to reduce luciferase activity by 50%.

Cytotoxicity assay

HEK293T cells (1.5×10^4) were seeded in 96-well plates for 20 h. A 2-fold dilution series of ivermectin was added to the cells, with five wells being used in parallel. After 72 h, the cells were incubated with CCK-8 reagent (Beyotime Biotechnology) for 30 min at 37 °C. The absorbance of each well at 450 and 600 nm was measured using the PerkinElmer EnSight microplate reader.

Statistical analysis

Statistical analysis was performed using GraphPad Prism. Two-tailed Student's *t*-tests were used for comparisons between two groups. For comparisons among three or more groups, a one-way analysis of variance (ANOVA) was conducted. Data are presented as means ± SD. Differences were considered statistically significant at *, $P < 0.05$, **, $P < 0.01$, ***, $P < 0.001$.

DATA AVAILABILITY

All data relevant to the study are included in the article or have been uploaded as supplementary information.

ETHICS STATEMENT

This article does not contain any studies with human or animal subjects performed by any of the authors.

AUTHOR CONTRIBUTIONS

Jielin Tang, Xinwen Chen, and Qi Yang conceived and designed the experiments; Jielin Tang, Xinwen Chen, Sijie Chen, Qi Yang, Yi Zhong, Yijun Deng, Junjun Liu, Jiyuan Xu, Bao Xue, and Fan Wang carried out the experiments and analyzed the data; Dan Huang and Yi Zheng contributed to the Southern blotting assay; Junjun Liu and Yuan Zhou helped with project management; Hanzhong Wang contributed to critical discussion and provided the pHBoV1-WH expression plasmid; Jielin Tang, Xinwen Chen, and Qi Yang wrote the manuscript.

CONFLICT OF INTEREST

Prof. Xinwen Chen is an editorial board member for *Virologica Sinica* and was not involved in the editorial review or the decision to publish this article. The authors declare that they have no conflict of interest.

ACKNOWLEDGEMENTS

We are grateful to the Core Facility Center of Guangzhou Laboratory for their continuous and generous support. We thank H. Z. Wang and W. X. Guan (Wuhan Institute of Virology) for providing the pHBoV1-WH expression plasmid. We thank R. J. Pei (Wuhan Institute of Virology) for the support in Southern blot experiment. We also thank H. Y. Li for her excellent technical support in ultrathin sectioning and negative-stain electron microscopy. This study was supported by the Guangzhou National Laboratory (SRPG22-002 to X. W. Chen), the Pearl River Talent Recruitment Program (2019CX01Y422 to X. W. Chen), the Natural Science Foundation of Guangdong Province (2025A1515011018 to J. L. Tang), and the Basic and Applied Basic Research Projects of Guangzhou Basic Research Program (2025A04J5492 to J. L. Tang, 2023A04J0161 to Q. Yang).

APPENDIX A. SUPPLEMENTARY DATA

Supplementary data to this article can be found online at https://doi.org/10.1016/j.virs.2025.03.009.

REFERENCES

Alvisi, G., Manaresi, E., Cross, E.M., Hoad, M., Akbari, N., Pavan, S., Ariawan, D., Bua, G., Petersen, G.F., Forwood, J., Gallinella, G., 2023. Importin α/β-dependent nuclear transport of human parvovirus b19 nonstructural protein 1 is essential for viral replication. Antivir. Res. 213, 105588.

Bonvicini, F., Bua, G., Manaresi, E., Gallinella, G., 2015. Antiviral effect of cidofovir on parvovirus B19 replication. Antivir. Res. 113, 11–18.

Bonvicini, F., Bua, G., Manaresi, E., Gallinella, G., 2016. Enhanced inhibition of parvovirus b19 replication by cidofovir in extendedly exposed erythroid progenitor cells. Virus Res. 220, 47–51.

Christensen, A., Kesti, O., Elenius, V., Eskola, A.L., Døllner, H., Altunbulakli, C., Akdis, C.A., Söderlund-Venermo, M., Jartti, T., 2019. Human bocaviruses and paediatric infections. Lancet Child Adolesc. Health 3, 418–426.

Colazo Salbetti, M.B., Boggio, G.A., Moreno, L., Adamo, M.P., 2023. Human bocavirus respiratory infection: tracing the path from viral replication and virus-cell interactions to diagnostic methods. Rev. Med. Virol. 33, e2482.

Deng, X., Xu, P., Zou, W., Shen, W., Peng, J., Liu, K., Engelhardt, J.F., Yan, Z., Qiu, J., 2017. DNA damage signaling is required for replication of human bocavirus 1 DNA in dividing hek293 cells. J. Virol. 91, e01831-16.

Dijkman, R., Koekkoek, S.M., Molenkamp, R., Schildgen, O., van der Hoek, L., 2009. Human bocavirus can be cultured in differentiated human airway epithelial cells. J. Virol. 83, 7739–7748.

Dixon, A.S., Schwinn, M.K., Hall, M.P., Zimmerman, K., Otto, P., Lubben, T.H., Butler, B.L., Binkowski, B.F., Machleidt, T., Kirkland, T.A., Wood, M.G., Eggers, C.T., Encell, L.P., Wood, K.V., 2016. Nanoluc complementation reporter optimized for accurate measurement of protein interactions in cells. ACS Chem. Biol. 11, 400–408.

Eyre, N.S., Johnson, S.M., Eltahla, A.A., Aloi, M., Aloia, A.L., McDevitt, C.A., Bull, R.A., Beard, M.R., 2017. Genome-wide mutagenesis of dengue virus reveals plasticity of the NS1 protein and enables generation of infectious tagged reporter viruses. J. Virol. 91, e01455-17.

Ghietto, L.M., Toigo D'Angelo, A.P., Viale, F.A., Adamo, M.P., 2017. Human bocavirus 1 infection of caco-2 cell line cultures. Virology 510, 273–280.

Heaton, N.S., Leyva-Grado, V.H., Tan, G.S., Eggink, D., Hai, R., Palese, P., 2013. In vivo bioluminescent imaging of influenza a virus infection and characterization of novel cross-protective monoclonal antibodies. J. Virol. 87, 8272–8281.

Huang, Q., Deng, X., Yan, Z., Cheng, F., Luo, Y., Shen, W., Lei-Butters, D.C., Chen, A.Y., Li, Y., Tang, L., Söderlund-Venermo, M., Engelhardt, J.F., Qiu, J., 2012. Establishment of a reverse genetics system for studying human bocavirus in human airway epithelia. PLoS Pathog. 8, e1002899.

Ishida, K., Noguchi, T., Kimura, S., Suzuki, H., Ebina, H., Morita, E., 2023. Tracking of human parvovirus b19 virus-like particles using short peptide tags reveals a membrane-associated extracellular release of these particles. J. Virol. 97, e0163122.

Kailasan, S., Garrison, J., Ilyas, M., Chipman, P., McKenna, R., Kantola, K., Söderlund-Venermo, M., Kučinskaitė-Kodzė, I., Žvirblienė, A., Agbandje-McKenna, M., 2016. Mapping antigenic epitopes on the human bocavirus capsid. J. Virol. 90, 4670–4680.

Mietzsch, M., Kailasan, S., Garrison, J., Ilyas, M., Chipman, P., Kantola, K., Janssen, M.E., Spear, J., Sousa, D., McKenna, R., Brown, K., Söderlund-Venermo, M., Baker, T., Agbandje-McKenna, M., 2017. Structural insights into human bocaparvoviruses. J. Virol. 91, e00261-17.

Mohammadi, M., 2023. Hbov-1: virus structure, genomic features, life cycle, pathogenesis, epidemiology, diagnosis and clinical manifestations. Front. Cell. Infect. Microbiol. 13, 1198127.

Nagashima, S., Primadharsini, P.P., Nishiyama, T., Takahashi, M., Murata, K., Okamoto, H., 2023. Development of a hibit-tagged reporter hepatitis e virus and its utility as an antiviral drug screening platform. J. Virol. 97, e0050823.

Nagashima, S., Takahashi, M., Kobayashi, T., Tanggis, Nishizawa, T., Nishiyama, T., Primadharsini, P.P., Okamoto, H., 2017. Characterization of the quasi-enveloped hepatitis e virus particles released by the cellular exosomal pathway. J. Virol. 91, e00822-17.

Qiu, J., Cheng, F., Burger, L.R., Pintel, D., 2006. The transcription profile of aleutian mink disease virus in crfk cells is generated by alternative processing of pre-mrnas produced from a single promoter. J. Virol. 80, 654–662.

Schildgen, V., Longo, Y., Pieper, M., Schildgen, O., 2018. T84 air-liquid interface cultures enable isolation of human bocavirus. Influenza Other Respir. Viruses 12, 667–668.

Shan, T.L., Cui, L., Dai, X.Q., Guo, W., Shang, X.G., Yu, Y., Zhang, W., Kang, Y.J., Shen, Q., Yang, Z.B., Zhu, J.G., Hua, X.G., 2010. Sequence analysis of an isolate of minute virus of canines in China reveals the closed association with bocavirus. Mol. Biol. Rep. 37, 2817–2820.

Shao, L., Shen, W., Wang, S., Qiu, J., 2021. Recent advances in molecular biology of human bocavirus 1 and its applications. Front. Microbiol. 12, 696604.

Shen, W., Deng, X., Zou, W., Engelhardt, J.F., Yan, Z., Qiu, J., 2016. Analysis of cis and trans requirements for DNA replication at the right-end hairpin of the human bocavirus 1 genome. J. Virol. 90, 7761–7777.

Shen, W., Deng, X., Zou, W., Cheng, F., Engelhardt, J.F., Yan, Z., Qiu, J., 2015. Identification and functional analysis of novel nonstructural proteins of human bocavirus 1. J. Virol. 89, 10097–10109.

Soldwedel, S., Demuth, S., Schildgen, O., 2024. T84 monolayer cell cultures support productive hbov and hsv-1 replication and enable in vitro co-infection studies. Viruses 16, 773.

Sumiyadorj, A., Murai, K., Shimakami, T., Kuroki, K., Nishikawa, T., Kakuya, M., Yamada, A., Wang, Y., Ishida, A., Shirasaki, T., et al., 2022. A single hepatitis b virus genome with a reporter allows the entire viral life cycle to be monitored in primary human hepatocytes. Hepatol. Commun. 6, 2441–2454.

Tamura, T., Igarashi, M., Enkhbold, B., Suzuki, T., Okamatsu, M., Ono, C., Mori, H., Izumi, T., Sato, A., Fauzyah, Y., Okamoto, T., Sakoda, Y., Fukuhara, T., Matsuura, Y., 2019. *In vivo* dynamics of reporter flaviviridae viruses. J. Virol. 93, e01191-19.

Tamura, T., Fukuhara, T., Uchida, T., Ono, C., Mori, H., Sato, A., Fauzyah, Y., Okamoto, T., Kurosu, T., Setoh, Y.X., Imamura, M., Tautz, N., Sakoda, Y., Khromykh, A.A., Chayama, K., Matsuura, Y., 2018. Characterization of recombinant flaviviridae viruses possessing a small reporter tag. J. Virol. 92, e01582-17.

Tang, J., Chen, S., Deng, Y., Liu, J., Huang, D., Fu, M., Xue, B., Liu, C., Wu, C., Wang, F., Zhou, Y., Yang, Q., Chen, X., 2025. Ma104 cell line is permissive for human bocavirus 1 infection. J. Virol. 25, e0153924.

Tang, J., Xu, C., Fu, M., Liu, C., Zhang, X., Zhang, W., Pei, R., Wang, Y., Zhou, Y., Chen, J., Miao, Z., Pan, G., Yang, Q., Chen, X., 2023. Sterile 20-like kinase 3 promotes tick-borne encephalitis virus assembly by interacting with ns2a and prm and enhancing the ns2a-ns4a association. J. Med. Virol. 95, e28610.

Tran, V., Moser, L.A., Poole, D.S., Mehle, A., 2013. Highly sensitive real-time in vivo imaging of an influenza reporter virus reveals dynamics of replication and spread. J. Virol. 87, 13321–13329.

Trapani, S., Caporizzi, A., Ricci, S., Indolfi, G., 2023. Human bocavirus in childhood: a true respiratory pathogen or a "passenger" virus? A comprehensive review. Microorganisms 11, 1243.

Yu, R., Li, X., Zhang, P., Xu, M., Zhao, J., Yan, J., Qiu, Chenli, Shu, J., Zhang, S., Kang, Miaomiao, Zhang, X., Xu, J., Zhang, S., 2024. Integration of hibit into enteroviruses: a universal tool for advancing enterovirus virology research. Virol. Sin. 39, 422–433.

Zhang, C., Zhang, G., Zhang, Y., Lin, X., Zhao, X., Cui, Q., Rong, L., Du, R., 2023. Development of an HiBit-tagged reporter H3N2 influenza a virus and its utility as an antiviral screening platform. J. Med. Virol. 95, e28345.

Zhu, J., Liu, Y., Luo, R., Feng, X., Li, Y., 2019. [Establishment of stable cell line expressing human bocavirus type 1 non-structural protein NS1 and its trans-transcriptional activation]. Sheng Wu Gong Cheng Xue Bao 35, 1126–1134.